NPHYS-2008-06-00736

Supplementary Information for

"Linear-*T* resistivity and change in Fermi surface at the pseudogap critical point of a high-T_c superconductor"

R. Daou [1], Nicolas Doiron-Leyraud [1], David LeBoeuf [1], S.Y. Li [1], Francis Laliberté [1], Olivier Cyr-Choinière [1], Y.J. Jo [2], L. Balicas [2], J.-Q. Yan [3], J.-S. Zhou [3], J.B. Goodenough [3] & Louis Taillefer [1,4]

1 Département de physique and RQMP, Université de Sherbrooke, Sherbrooke, Québec J1K 2R1, Canada

2 National High Magnetic Field Laboratory, Florida State University, Tallahassee, Florida 32306, USA

3 Texas Materials Institute, University of Texas at Austin, Austin, Texas 78712, USA

4 Canadian Institute for Advanced Research, Toronto, Ontario M5G 1Z8, Canada

METHODS

In-plane samples. The two samples of Nd-LSCO used for in-plane transport were grown using a traveling float zone technique in an image furnace, as described in ref. 1. The nominal Sr concentration for the two growths was $x = 0.20$ and $x = 0.25$, respectively. The actual doping p of small crystals cut out of the resulting large boules is expected to be $p = x \pm 0.01$. The physical dimensions of the samples cut out of the single-crystal boules were measured using an optical microscope and are shown in Table 1.

Table 1

Sample (in-plane)	**Length, *L* [mm]**	**Width, *w* [mm]**	**Thickness, *t* [mm]**
Nd-LSCO x=0.20	1.51 ± 0.05	0.50 ± 0.02	0.64 ± 0.02
Nd-LSCO x=0.25	2.50 ± 0.05	0.51 ± 0.02	0.51 ± 0.02

***c*-axis sample**. One sample of Nd-LSCO was used for *c*-axis resistivity, shown in Fig. 2b. It was cut from the same $x = 0.25$ boule as the $x = 0.25$ in-plane sample. It had a resistive $T_c = 17 \pm 0.5$ K in zero field.

Superconducting transition temperature T_c. The superconducting transition temperature T_c of our Nd-LSCO in-plane samples was determined via magnetic susceptibility measurements in a SQUID magnetometer. T_c is defined as the midpoint of the transition and the width is that of the susceptibility drop between 90 % and 10 %. In Table 2, these T_c values are compared with T_c defined as the temperature where the resistivity goes to zero.

Table 2

Sample (in-plane)	**T_c [K] (midpoint)**	**T_c [K] (width)**	**T_c [K] (ρ = 0)**
Nd-LSCO x=0.20	19	9	20.5 ± 0.5
Nd-LSCO x=0.25	13	8	17.0 ± 0.5

Hole doping *p*. By comparing the T_c values and the absolute values of the resistivity (at 250 K) in each of our two in-plane samples (in bold) with previous measurements on Nd-LSCO and LSCO (for which we assume $p = x$), we arrive at an estimate of the doping, given in Table 3.

Table 3

Sample	**x**	**Tc (ρ = 0)**	**ρ (T = 250 K) [μΩ cm]**	**p**	**Ref.**
Nd-LSCO	0.20	20 ± 0.5	232 ± 20	0.20	[2,3]
LSCO	0.20	N/A	210 ± 20	0.20	[3]
LSCO	0.20	N/A	230 ± 20	0.20	[4]
Nd-LSCO	**0.20**	**20.5 ± 0.5**	**237 ± 20**	**0.20 ± 0.005**	**This work**
LSCO	0.22	N/A	192 ± 20	0.22	[4]
Nd-LSCO	**0.25**	**17.0 ± 0.5**	**164 ± 15**	**0.24 ± 0.005**	**This work**
Nd-LSCO	0.25	7 ± 0.5	132 ± 13	0.25	[2,3]
LSCO	0.25	N/A	116 ± 12	0.25	[3]

Contacts. Electrical contacts on the Nd-LSCO samples were made to the crystal surface using Epo-Tek H20E silver epoxy. This epoxy was cured for 5 min at 180 C, then annealed at 500 C in flowing oxygen for 1 hr so that the silver diffused into the surface. This resulted in contact resistances of less than 0.1 Ω at room temperature. The contacts were wrapped around all four sides of the sample. In addition, the current contacts covered the end faces. Hall contacts were placed opposite each other in the middle of the samples, extending along the length of the *c*-axis, on the sides. The uncertainty in the quoted length (between contacts) of the sample, and hence the geometric factor, reflects the width of the voltage contacts.

Magnetic field direction. In all measurements, the magnetic field was applied along the *c*-axis of the sample.

Measurements of resistivity and Hall coefficient. The resistivity $\rho(T) \equiv R_{xx}\, w\, t / L$ and Hall coefficient $R_H(T) \equiv R_{xy}\, t / H$ of each in-plane sample were measured using the standard six-terminal AC technique. A resistance bridge or a lock-in amplifier was used to measure the resistance. Field reversal was used to obtain the symmetric and anti-symmetric parts of the voltages, accounting for any misalignment of the contacts. Therefore, the longitudinal (R_{xx}) and transverse (R_{xy}) resistances were obtained as follows:

$$R_{xx} = (R(B) + R(-B)) / 2 \quad \text{and} \quad R_{xy} = (R(B) - R(-B)) / 2.$$

Low-field measurements were performed in Sherbrooke, in the temperature range 4-300 K using a steady magnetic field of up to 15 T. High-field measurements on the same samples were performed at the NHMFL in Tallahassee, in a helium-3 refrigerator in DC fields of up to 33 T (R_{xy} for the $x = 0.20$ sample and R_{xx} for the $x = 0.25$ sample) and 35 T (R_{xx} for the $x = 0.20$ sample).

The resistivity $\rho_c(T)$ of the *c*-axis sample shown in Fig. 2b was measured at the NHMFL using a standard four-terminal technique, in a field of 30 T.

No dependence on magnetic field was observed in either the resistance R_{xx} or the Hall coefficient $R_H = t\,R_{xy} / B$. Fig. S1 shows the separate data taken at $H = 0$ and $H = 15$ T in Sherbrooke and at $H = 35$ T in Tallahassee on sample $x = 0.20$ ($p = 0.20$); one can see that there is negligible magneto-resistance (in the normal state).

Hall effect data taken at the NHMFL (up to 33 T) on the $x = 0.20$ sample had a low signal-to-noise ratio. The data shown in Fig. 4 was smoothed by a running average of width 100 data points (taken very densely). In addition, a small offset of 10 % was recorded between the Sherbrooke data at 15 T and the NHMFL data at 33 T in the temperature region of overlap (15-25 K). In Fig. 4, the NHMFL data was normalized to match the lower-noise Sherbrooke results. This is justified given the absence of field dependence in both R_{xx} and R_H up to 35 T.

Determination of *T**. The pseudogap temperature *T** is defined as the point where the resistivity deviates from its high-temperature linear behavior. In Fig. S2, we show how it can be obtained readily by plotting $\rho(T) - (\rho_0 + AT)$ versus temperature, where $(\rho_0 + AT)$ is a fit to the high-temperature region. The *T** values thus obtained are plotted vs doping in Fig. 3. Data on LSCO at $p = 0.14$ (from ref. 4) is also shown for comparison.

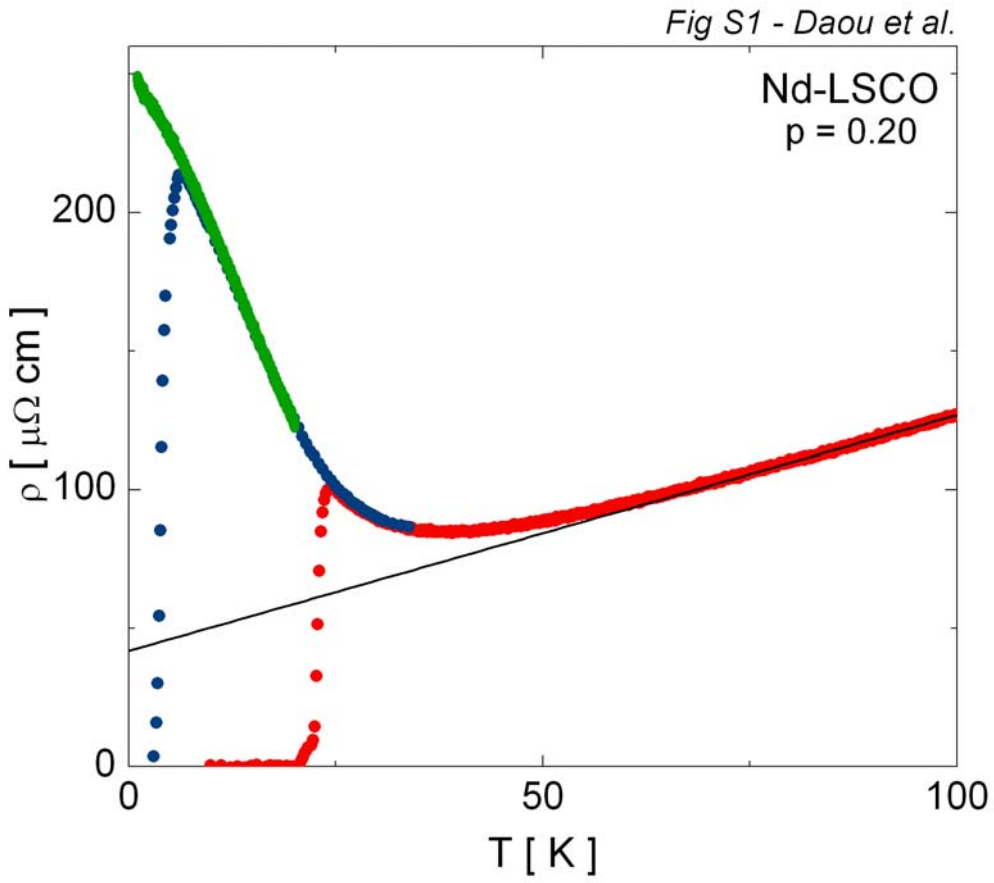

Figure S1 | Electrical resistivity of Nd-LSCO at *p* = 0.20.

Temperature dependence of the in-plane electrical resistivity, $\rho_{ab}(T)$, for the in-plane Nd-LSCO sample with $x = 0.20$ ($p = 0.20$), at three different magnetic fields: $H = 0$ (red), $H = 15$ T (blue), and $H = 35$ T (green). The fact that all three curves overlap almost perfectly (in the normal state) shows that there is negligible magneto-resistance. This implies that the effect of a magnetic field is simply to remove superconductivity, without altering the underlying normal state. The data shown in Fig. 1 and Fig. 2a includes all three sets of data.

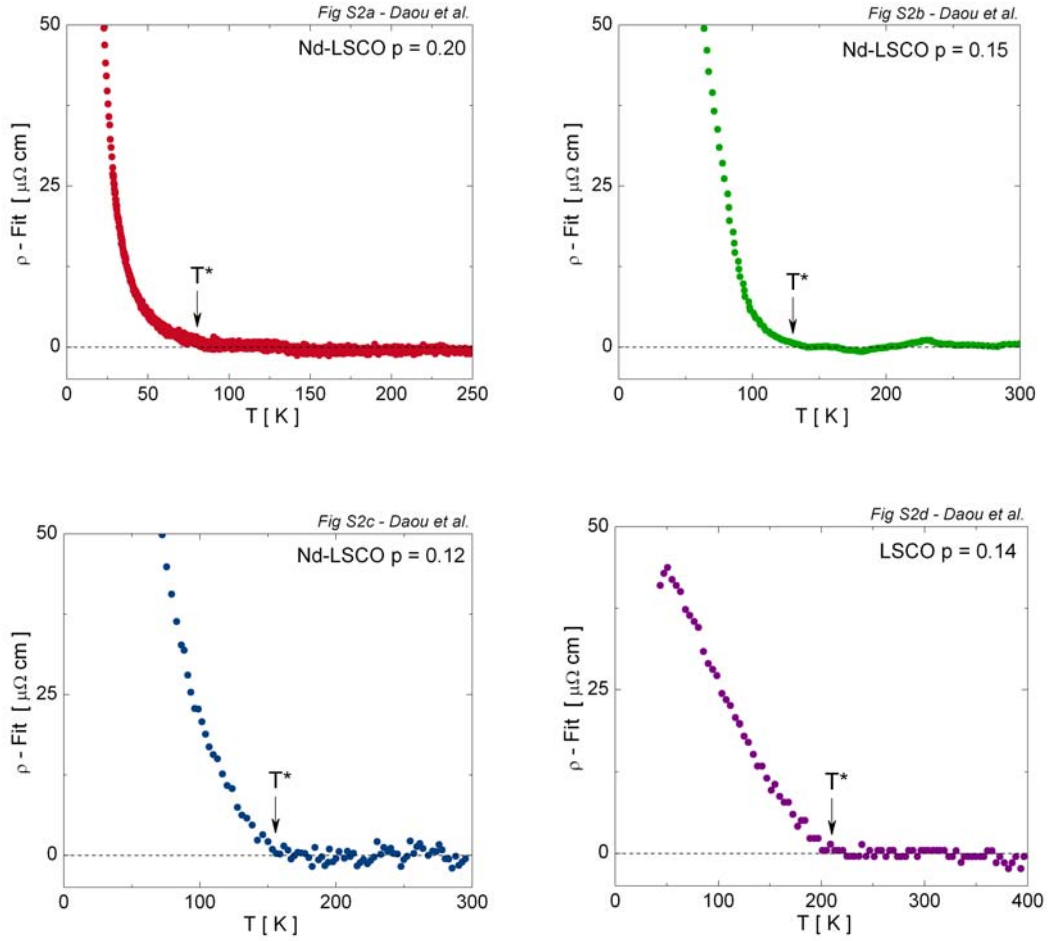

Figure S2 | Pseudogap temperature in Nd-LSCO and LSCO.

Resistivity $\rho(T)$ minus a linear fit to the high-temperature data of the form $\rho_0 + AT$. **a)** Nd-LSCO at $p = 0.20$ (this work); **b)** Nd-LSCO at $p = 0.15$ (from ref. 2); **c)** Nd-LSCO at $p = 0.12$ (from ref. 2). This allows us to define the pseudogap temperature T^* as the end of the linear-T regime at high temperature. The values obtained are $T^* = 80$, 130, and 155 K, respectively, with an error bar of about ± 15 K in all cases. They are plotted on a p – T phase diagram in Fig. 3. **d)** LSCO at $p = 0.14$ (from ref. 4). This shows that the onset of the pseudogap has a similar signature in the resistivity of LSCO and Nd-LSCO, with comparable T^* values.

[1] Yan, J.-Q. *et al*., *Phys. Rev. B* **68**, 104520 (2003).

[2] Ichikawa, N. *et al*., *Phys. Rev. Lett.* **85**, 1738-1741 (2000).

[3] Ichikawa, N. Ph.D. Thesis (University of Tokyo, 1999).

[4] Ando, Y. *et al*., *Phys. Rev. Lett.* **93**, 267001 (2004).